Open Archive TOULOUSE Archive Ouverte (OATAO)

OATAO is an open access repository that collects the work of Toulouse researchers and makes it freely available over the web where possible.

Cyclic Voltammetric Experiment - Simulation Comparisons of the Complex Mechanism Associated with Electrochemical Reduction of Zr^{4+} in LiCl-KCl Eutectic Molten Salt

Cesimiro P. Fabian,[a,b,*,z] **Vittorio Luca,**[c] **Thanh H. Le,**[d] **Alan M. Bond,**[d,*] **Pierre Chamelot,**[e] **Laurent Massot,**[e] **Concepción Caravaca,**[f] **Tracey L. Hanley,**[a] **and Gregory R. Lumpkin**[a]

[a]*Institute of Materials Engineering, Australian Nuclear Science and Technology Organisation, Locked Bag 2001 Kirrawee DC NSW 2232, Lucas Heights NSW 2234, Australia*
[b]*Research & Innovations in Electrometallurgy & Consulting, Geebung QLD 4034, Australia*
[c]*Programa Nacional de Gestión de Residuos Radioactivos, Comisión Nacional de Energía Atómica, 1650 San Martin, Buenos Aires, Argentina*
[d]*School of Chemistry, Monash University, Clayton, Victoria 3800, Australia*
[e]*Procédés Electrochimiques, Université Paul Sabatier, 31062 Toulouse, Cedex 4, France*
[f]*Departamento de Fisión Nuclear, Centro de Investigaciones Energéticas, Medioambientales y Tecnológicas, 28040 Madrid, Spain*

Nuclear energy increasingly represents an important option for generating largely clean CO$_2$-free electricity and zirconium is a fission product that is expected to be present in irradiated fuels. The present investigation addresses the electrochemical reduction of Zr^{4+} to Zr^o in LiCl - KCl eutectic molten salt in the temperature range 425–550°C using cyclic voltammetry (CV), square-wave voltammetry (SWV) and bulk electrolysis. Simulations of the CV data indicate that the initial reduction proceeds through surface confined steps: Zr^{4+*} + 2e$^-$ ↔ Zr^{2+*} and Zr^{2+*} + 2e$^-$ ↔ Zr* processes (* adsorbed species) followed by a peak-shaped complex diffusion controlled step that consists of a combination of closely spaced processes associated with the reactions Zr^{4+} + 4e$^-$ → Zr^o and Zr^{4+} + 3e$^-$ → Zr^{+*}. Zr^{+*}, probably in the form of ZrCl* is then further reduced to Zr^{o*} at even more negative potentials. The simulations provide the first quantitative analysis of the thermodynamics and kinetics of the Zr^{4+} reduction in the LiCl-KCl eutectic.

Pyroelectrochemical processes based on molten chloride or fluoride electrolyte systems have over the past decade received substantial interest for the reprocessing of irradiated nuclear fuel. The renewed interest owes its origin to several attractive features of the pyroelectrochemical approach in comparison to hydrometallurgical reprocessing.[1] Advantages include: 1) the ability to handle different fuel types, i.e., metal, oxide, carbide, nitride, mixed ceramic-metal, ceramic-coated particles; 2) potential for reprocessing freshly irradiated fuel without the need for fuel cooling; 3) small plant footprint compared with hydrometallurgical reprocessing; 4) the absence of organic solvents and 5) favorable criticality, safety and proliferation resistance.[2] Zirconium, a fission product, our material of interest in this paper, is expected to be present in irradiated fuels.

Pyroelectrochemical reprocessing strategies are particularly applicable to the reprocessing of sodium cooled fast reactor fuel. The potential of this approach has been demonstrated by the Idaho National Laboratory (INL) where 50 tons of sodium-bonded Experimental Breeder Reactor (EBR II) fuel have been processed using LiCl – KCl eutectic molten salt. Moreover, European, Japanese and Korean efforts in pyrochemistry have focused on uranium, plutonium, and complete minor actinide (MA) recovery. Recycling of MAs requires separation from the radio-lanthanides present in the irradiated fuel. Hence, considerable effort has been devoted to this issue, especially for the LiCl-KCl eutectic (51:49 mol%) system.

Since zirconium is a major component in reactor fuel types such as U-Zr and U-Pu-Zr,[3] in a pyro-electrometallurgical reprocessing context, it is reasonable to expect that a proportion of zirconium could be carried over into a molten salt electrolyte and as such could interfere with the recovery of actinides.[4] For example, the presence of zirconium in LiCl-KCl eutectic molten salt containing actinide ions appears to interfere with the separation of U^{3+} due to the proximity of their electrode potentials and alloy formation.[5,6]

Clearly in order to advance pyroelectrochemical techniques in reactor fuel applications, detailed knowledge on the electrochemical reactivity of zirconium in molten salt media is needed. While there are several studies on the electrochemistry of Zr^{4+} in LiCl-KCl eutectic melt, details of reaction mechanism are still unclear due to the low

sublimation point (331°C) and hygroscopic behavior of ZrCl$_4$, and the complex electrochemical behavior which consists of a series of stepwise processes. In 1965, Baboian et al.[7] studied the electrochemistry of Zr^{4+} in LiCl-KCl eutectic molten salt using potentiometric and polarographic techniques. These authors indicated that Zr^{4+} is the predominant species and suggested that the Zr^{4+}/Zr^o electrode potential is −1.22 V while that of the Zr^{2+}/Zr^o process is −1.12 V (vs. Ag(I)/Ag) at 550°C. Electrorefining of zirconium in LiCl-KCl eutectic molten salt also was studied by Kipouros et al.[8] These authors indicated that the predominant cathodic reaction occurs as in, Equation 1

$$ZrCl_6^{2-} + 4e^- \rightarrow Zr^o(s) + 6Cl^- \qquad [1]$$
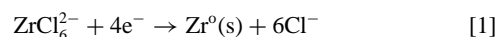
but also noted that side reactions such as Zr^{4+} + Zr^o → Zr$^+$ + Zr^{2+} (or Zr^{3+}) and their combinations could reduce the current efficiency. Baboian et al.[7] suggested the irreversible comproportionation reaction, (Equation 2) could occur when the electrolyte is heated and cooled between 450 and 550°C whereas Basile et al.[9] described this process in the context of an equilibrium reaction.

$$Zr^{4+} + Zr^o \rightarrow 2Zr^{2+} \qquad [2]$$

Sakamura[4] studied the cyclic voltammetry of zirconium in the LiCl-KCl eutectic molten salt at temperatures over the range 450 to 550°C using Mo as the working electrode. The initial process at about −1.0 V (vs. Ag/AgCl) was assumed to correspond to the reaction given in Equation 3

$$Zr^{4+} + 2e^- \rightarrow Zr^{2+} \qquad [3]$$

A process observed at about −1.2 V (vs. Ag/AgCl) at 500°C was postulated to correspond to the reduction of Zr^{4+} to Zr^o and ZrCl as in Equations 4 and 5.

$$Zr^{4+} + 4e^- \rightarrow Zr^o \qquad [4]$$

$$Zr^{4+} + 3e^- \rightarrow ZrCl \qquad [5]$$
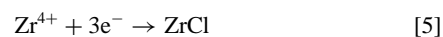
Sakamura[4] described ZrCl, proposed in Equation 5, as a product of reduction of Zr^{4+} as being 'insoluble' and 'metastable' in the molten salt and supported this hypothesis with electrowinning tests. Furthermore, it was noted that ZrCl may be reduced to Zr^o at potentials more negative than −1.3 V (vs. Ag/AgCl).

A recent voltammetric and chronopotentiometric (CP) study by Ghosh et al.[10] confirmed the presence of processes described by Sakamura.[4] Additional observations were that CV data are complicated by adsorption of Zr^{2+} at the tungsten-working electrode, and CP transients exhibited two transition plateaus that were said to correspond to Zr^{4+}/Zr^{2+} and Zr^{2+}/Zr^o reductions.

In summary, from the literature reviewed above, it may be concluded that the reduction of Zr^{4+} to Zr^o in molten salt media takes place in a series of electron transfer steps such as Zr^{4+}/Zr^{2+}, Zr^{2+}/Zr^o and Zr^{2+}/Zr^+, with comproportionation reactions such as $Zr^{4+} + Zr^o \rightarrow Zr^+ + Zr^{2+}$ (or Zr^{3+}) and adsorption also being important. However, the papers published on the subject provide only limited qualitative forms of analysis of the complex electrochemical reduction of zirconium. The aim of the present study therefore is to probe the reaction mechanism for zirconium electroreduction in LiCl-KCl eutectic molten salt using cyclic voltammetry, square-wave voltammetry and bulk electrolysis. In particular, a comprehensive attempt at simulation of the CV data has been undertaken in order to extract quantitative thermodynamic and electrokinetic details for the first time. The use of simple simulations was introduced by Fabian et al.[11] in studies on the reduction of La^{3+} in LiCl-KCl eutectic molten salt, but the concept has now been extended to accommodate coupled chemical reactions and adsorption in the case of reduction of Zr^{4+}.

Experimental

High purity LiCl (Aldrich, 99%) and KCl (Merck, 99.999%) were used to prepare the eutectic melt (59% mol LiCl and 41% mol KCl; 65 g of the salt mixture). Known wt% masses of zirconium chloride, $ZrCl_4$ (Sigma-Aldrich, 99.99%) were added to the eutectic salt, but ICP analysis was used to determine the exact concentrations in the bath. The reactor head consisted of an 8-port borosilicate ground glass vacuum flange. All components were dried at 80°C for at least 12 h prior to assembly. The working electrode (WE) was a 1 mm diameter tungsten wire (W), with the bottom-end rounded off to form a hemicylinder. The oxide layer on a WE was removed with 4000 grit SiC paper, then rinsed with dilute nitric acid and distilled water and dried for least 1 h at 80°C. After about one hour of use, the WE was cleaned once again with the SiC paper and ethanol and then used again. The counter electrode (CE) was a 3 mm diameter x 400 mm glassy carbon rod (SIGRADUR G) encased in an alumina tube of 6 mm OD. The Ag/AgCl reference electrode (REF) was constructed from 0.75 mol kg^{-1} AgCl dissolved in LiCl-KCl eutectic molten salt in contact with 1 mm diameter silver wire embedded in 6 mm OD x 4 ID x 300 mm quartz tubing sealed with high temperature epoxy resin. The temperature of the eutectic was monitored using a thermocouple (type K, ± 2°C) sheathed in alumina. The eutectic melt was weighed into a glassy carbon crucible (SIGRADUR G, GAZ 12; 50 mm OD x 85 mm H) in a nitrogen filled (< 1 ppm oxygen and water) glove box.

The electrochemical reactor was purged first with dry argon gas (99.99%), then sealed and evacuated to about 0.2 mbar. Further dehydration of the salt was undertaken by heating under vacuum at about 300°C for 72 h. After this time, the vacuum was removed and the vessel purged with argon. The temperature was then increased to 425 or 450°C and the zirconium chloride sample added. Numerous preliminary tests were conducted to reduce the sublimation of $ZrCl_4$ and HCl gas was not used under the conditions finally employed.

An AUTOLAB potentiostat PGSTAT302N from Eco Chimie, driven by Nova 1.6, 1.7 and GPES 4.9 software packages, was used to conduct all the electrochemical experiments. DigiElch 6 (build 12) was used to simulate the CV data. Multiple experiments employing different zirconium concentrations and sweep rates were imported into DigiElch and compared with simulated cyclic voltammograms to extract the required kinetic and thermodynamic properties.

The controlled potential electrolysis experiment, required for identification of ZrCl as a product of reduction, was conducted for about 1 h at -1.2 V (vs. Ag/AgCl) and 500°C with a 0.18 mol.kg^{-1} Zr^{4+} solution. This electrolysis potential lies just prior to the onset of the second step. The initial current of 20 mA, rather than decaying with time, gradually increased to 50 mA, possibly due to dendrite formation and a decrease in the working-reference electrode gap. The solid obtained on the working electrode was spongy, yellowish and pink in color. After removal from the electrode surface, the solid was mounted in an air-tight container under a nitrogen atmosphere, and transferred to a Bruker D8 diffractometer fitted with Cu tube and SOL-XE detector. Diffraction was acquired over an angular range of 2° to 120° two theta with a step size of 0.03 and a counting time of 10 seconds per point.

Results and Discussion

Experimental Aspects of the Cyclic Voltammetry of Zirconium.— If Nernstian reduction of Zr^{4+} to Zr^o were to occur in a voltammetric experiment, all steps involved in the reaction mechanism would appear to take place simultaneously so the reaction would equate to an overall Zr^{4+}/Zr^o process. However, if the lower Zr^{3+}, Zr^{2+} and/or Zr^+ states are stable and/or *adsorbed*, electron transfer may be found to take place in a series of consecutive and concurrent steps.

Sakamura[4] reported 13.5 mA current (WE area: 0.325 cm^2) from 0.00123 mole fraction ZrCl$_4$ (= 0.0171 mol.kg^{-1} Zr^{4+}) at 100 mVs^{-1} scan rate and 500°C. Preliminary experiments in the present study produced higher current densities and further studies suggested that low concentrations of electroactive zirconium ions formed in the molten bath and hence lower current densities might be attributable to ZrCl$_4$ and its hygroscopic behavior. Also, it is known that zirconium tetrachloride reacts readily with O_2^- ions to form ZrOCl$_2$ and ZrO$_2$ which can precipitate from the molten salt mixture.[12] Experimentsl data suggested that ZrOCl$_2$ and/or ZrO$_2$, once formed, are very difficult to dissolve and non-electroactive even after HCl$_{(g)}$ cleaning at 500°C. In the present studies, between 1.00 and 1.25% ZrCl$_4$ (w/w) was added to the bath and currents detected per unit of electrode area were higher than those reported by Sakamura[4] and it was assumed in this study that all zirconium is electroactive. The rest potential became more negative than -1 V (vs. Ag/AgCl) upon addition of ZrCl$_4$ greater than 1.25% (w/w).

A profile of the CV experimental data obtained for the reduction Zr^{4+} is presented in Figure 1a with a switching potential of -1.5 V (vs. Ag/AgCl). Two reduction steps are seen in this potential range. The first feature to note from perusal of Figure 1 is that as expected both cathodic processes vary systematically with temperature. That is, larger currents and reduction at less negative potentials is found at the higher temperatures. Moreover, the initial reduction process was more drawn out (segment AB), than the one obtained at more negative potentials (segment BC). The initial process may involve interaction
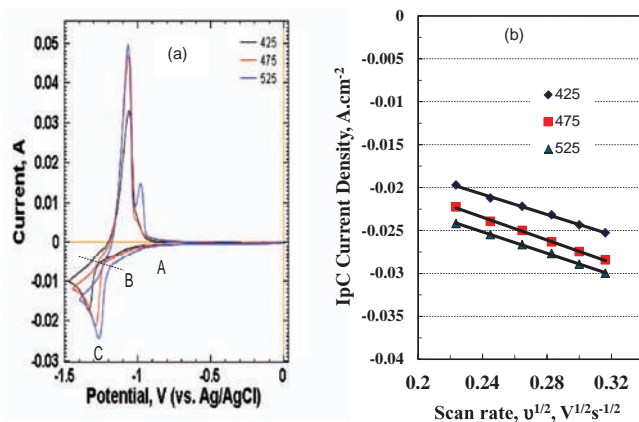

Figure 1. (a) Cyclic voltammograms obtained at 425, 475 and 525°C with a sweep rate of 100 mVs^{-1} in LiCl – KCl eutectic molten salt. [Zr^{4+}] = 0.0270 molkg^{-1}. WE: W wire (electrode area at: 425°C, 0.410; 475°C, 0.492 and 525°C, 0.507 cm^2); CE: - GC rod; REF, Ag/AgCl; [AgCl] = 0.75 molkg^{-1}. (b) Plot of peak current density for the second reduction process vs. square root of scan rate indicating that this process is diffusion-controlled.
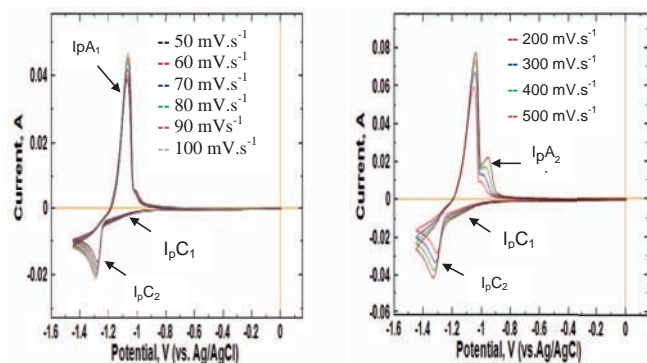
Figure 2. Cyclic voltammograms as a function of scan rate for reduction of Zr^{4+} (0.027 molkg^{-1}) in LiCl - KCl eutectic molten salt at 475°C. WE: W 1 mm dia. wire (electrode area: 0.492 cm^2); CE: - GC rod; REF, Ag/AgCl; [AgCl] = 0.75 molkg^{-1}.

Figure 4. Cyclic voltammograms as a function of scan rate for the reduction of Zr^{4+} (0.0445 molkg^{-1}) in LiCl - KCl eutectic molten salt at 500°C. WE: W 1 mm dia. wire (electrode area: 0.37 cm^2); CE: - GC rod; REF, Ag/AgCl; [AgCl] = 0.75 molkg^{-1}.

of the Zr^{4+} with the surface while the second peak shaped process is likely to be associated with diffusion. On reversing the potential scan direction after the second step, two oxidation processes are detected that are scan rate dependent (Figure 1). The symmetrical shape of these components implies oxidation of surface confined species.

Figure 1b provides a plot of peak current density vs. square root of the scan rate, $\upsilon^{1/2}$ for the second reduction process. The current increases linearly with the square root of scan rate as the Randles-Sevcik equation predicts, implying that this process is diffusion-controlled. Interestingly, Figure 1b also indicates that the difference in current between 475 and 425°C for this second reduction step is greater than that between 525 and 475°C. It is difficult to construct analytical theoretical models for complex reduction processes of this kind, so a practical approach is to compare the experimental behavior with the predictions derived from simulations.[13,14]

Figure 2 contains the scan rate dependence of cyclic voltammograms at 475°C with a Zr^{4+} concentration of 0.027 molkg^{-1} (1% wt mass ZrCl$_4$ added, 0.655 g) in LiCl - KCl eutectic molten salt and with a -1.45 V (vs. Ag/AgCl) switching potential. The cathodic (I_pC_1 and I_pC_2) and anodic (I_pA_2 and I_pA_1) components are designated in this Figure. Clearly, the first reduction step (I_pC_1) is very drawn out at all scan rates, implying that this reaction is predominantly surface based, in contrast to the second reduction step, which contains a diffusion component.

Figure 3 shows that the peak-to-peak separations ΔE_{pp} (ΔEpp = |E_p (anodic) – E_p (cathodic) |) for the second reduction process as a function of temperature and scan rate.

Figure 4 provides the scan rate dependence of cyclic voltammograms from 50 to 500 mVs^{-1} for the reduction of Zr^{4+} at a higher concentration of 0.0445 molkg^{-1} in LiCl - KCl (1.25% wt mass ZrCl$_4$ added, 0.869 g) eutectic molten salt at 500°C with a switching potential at -1.425 V (vs Ag/AgCl). Figure 5 shows the corresponding peak-to-peak separation potentials vs. scan rate plot as a function of temperature. The results of the cyclic voltammetric data can be summarized as follows: 1) The reduction of Zr^{4+} is well defined over the temperature range of 425 to 550°C (698 to 823 K) and concentration range of 0.027 to 0.045 molkg^{-1}, 2) reduction up to -1.45 V (vs. Ag/AgCl) consists of two major processes. The first reduction step, (IpC_1) probably includes a dominant adsorption component with the second process, (I_pC_2) having a dominant diffusion component; and 3) oxidation on reversing the scan direction is dominated by a large peak, I_pA_2 followed by a smaller process, I_pA_1. Sakamura[4] also reported predominantly *two anodic processes peaks* at 500°C using Mo as the WE with the first decreasing and the second increasing in relative importance as the scan rate is increased from 100 to 800 mVs^{-1} (vs. Ag/AgCl, Figure 4[4]).

Figure 5 also provides the peak-to-peak separation data derived from Figure 4 for the second process vs. scan rate. It can be deduced from analysis of Figures 3 and 5 that ΔEpp varies from 260–325 mV at 425°C to 156–217 mV at 550°C consistent with the overall irreversibility of this process.

The CV data presented in Figure 2 were obtained at 475°C with 0.027 molkg^{-1} of Zr^{4+}, while those in Figure 4 were obtained at 500°C with 0.0445 molkg^{-1}. Additional cyclic voltammetric experiments
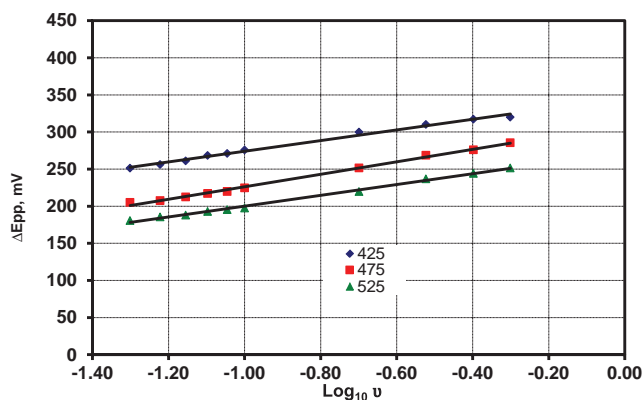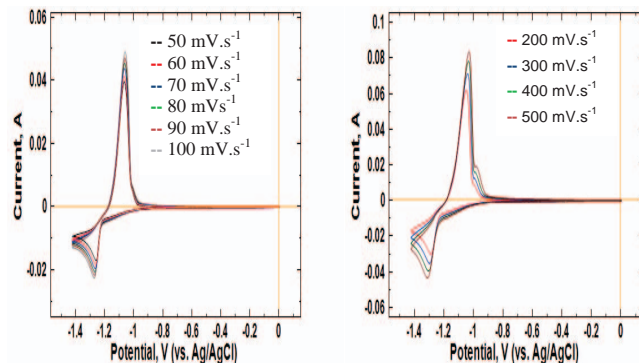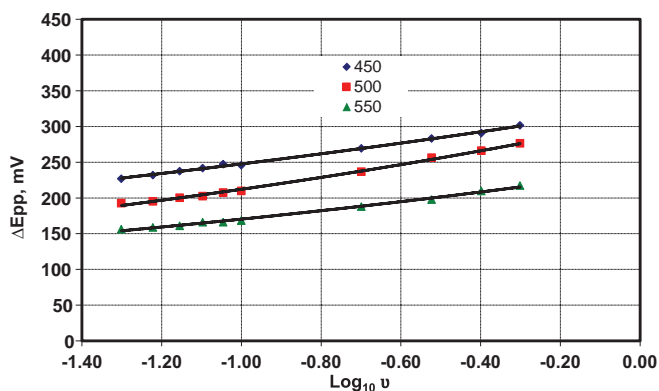

Figure 3. Plots of ΔE_{pp} vs. scan rate for the second Zr^{4+} reduction process at 425, 475 and 525°C in LiCl - KCl eutectic molten salt. [Zr^{4+}] = 0.027 molkg^{-1}, WE: W 1 mm dia. wire (electrode area: S_{425} = 0.410; S_{475} = 0.492; S_{525} = 0.507 cm^2); CE: - GC rod; REF, Ag/AgCl; [AgCl] = 0.75 molkg^{-1}.

Figure 5. Plots of ΔE_{pp} vs. scan rate for the second Zr^{4+} reduction process at 450, 500 and 550°C in LiCl - KCl eutectic molten salt. Zr^{4+} = 0.0445 molkg^{-1} at 450 and 500°C and 0.0460 mol.kg^{-1} at 550°C, WE: W wire (electrode area: S_{450} = 0.325; S_{500} = 0.370; S_{550} = 0.362 cm^2); CE: - GC rod; REF, Ag/AgCl; [AgCl] = 0.75 molkg^{-1}.
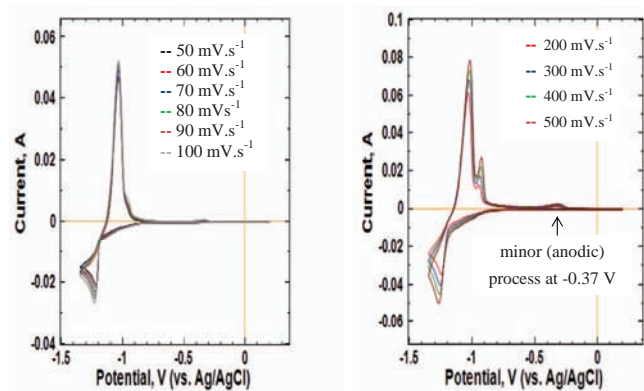
Figure 6. Examples of cyclic voltammograms showing the presence of a minor oxidation process occasionally detected at -0.37 V (Ag/AgCl). $[Zr^{4+}]$ = 0.0428 molkg^{-1} in LiCl - KCl eutectic molten salt at 525°C with area = 0.338 cm^2. WE: W 1 mm dia. wire; CE: - GC rod; REF, Ag/AgCl; [AgCl] = 0.75 molkg^{-1}.
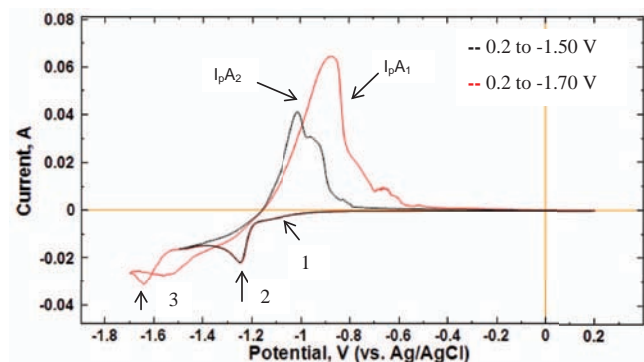

Figure 7. Comparison of cyclic voltammograms obtained at a scan rate of 100 mVs^{-1} with switching potentials at -1.5 and -1.7 V (vs. Ag/AgCl) at 500°C in LiCl - KCl eutectic molten salt. The presence of a third reduction process at about -1.64 V (vs. Ag/AgCl) is detected when the more negative switching potential is employed. $[Zr^{4+}]$ = 0.0428 molkg^{-1} with electrode area = 0.307 cm^2. WE: W 1 mm dia. wire; CE: - GC rod; REF, Ag/AgCl; [AgCl] = 0.75 molkg^{-1}.

were conducted with 0.0428 molkg^{-1} of Zr^{4+} at 475, 500, 525 and 550°C. Figure 6 shows results at 525°C with a switching potential of -1.375 V (vs Ag/AgCl). All the cathodic and anodic processes shown in this Figure and with the other conditions are consistent with those shown in Figures 2 and 4 in terms of relative shapes and characteristics.

Ghosh et al.[6,10] reported an additional anodic process at -0.37 V with a significant peak current (Figure 4, 0.0884 molkg^{-1} ZrCl$_4$ at 550°C) which was attributed to the reaction Zr^{2+} → Zr^{4+} + 2e$^-$. In the present work, the process assigned to this reaction is the one designated as IpA$_2$ which is well removed from -0.37 V (see details below). However, in this work, a minor process was occasionally observed at -0.37 V with high scan rates (Figure 6b) and is possibly associated with monolayer dissolution of zirconium oxide/oxychloride/Zr^{4+*}/ZrCl. Sakamura[4] avoided any possibility of detecting an anodic peak at -0.37 V since the initial and final potentials used in the cyclic voltammetry were -0.4 V (vs. Ag/AgCl). The variation in this process is probably due to the differences in salt treatments. Ghosh et al.[10] appears to have heated LiCl-KCl and ZrCl$_4$ together at 455°C under a chlorine gas atmosphere. Preliminary studies conducted in this work indicated that when the eutectic salt and ZrCl$_4$ are mixed before the drying process, oxygen monolayers present on the salt appear to readily react with ZrCl$_4$ even in the presence of vacuum and once zirconium oxychloride is formed it is difficult to dissolve even with HCl(g).[12]

Sakamura[4] reported a third reduction process when the switching potential was extended to even more negative values than considered to date. Figure 7 confirms the presence of additional reduction involving a nucleation-growth mechanism when the potential is switched at -1.7 V (vs. Ag/AgCl). Under these conditions, the second oxidation process I$_p$A$_2$ becomes greatly enhanced, relative to I$_p$A$_1$, implying that the product of the third and second reduction steps is common and presumably zirconium metal (Zr°). Thus, process I$_p$A$_2$ is attributed to stripping of zirconium metal from the electrode surface.

Controlled Potential Electrolysis.— XRD analysis in the 2θ range from 20 to 40 of the product formed by bulk electrolysis at -1.2 V (vs Ag/AgCl) (Figure 8) indicate the presence of amorphous material with the major diffraction component being attributable to the eutectic salt and ZrCl. The eutectic salt shows strong preferred orientation that precluded the observation of the 35 and 47.5 2θ degree peaks reported by Sakamura.[4] Chemical analyzes also indicated the presence of the
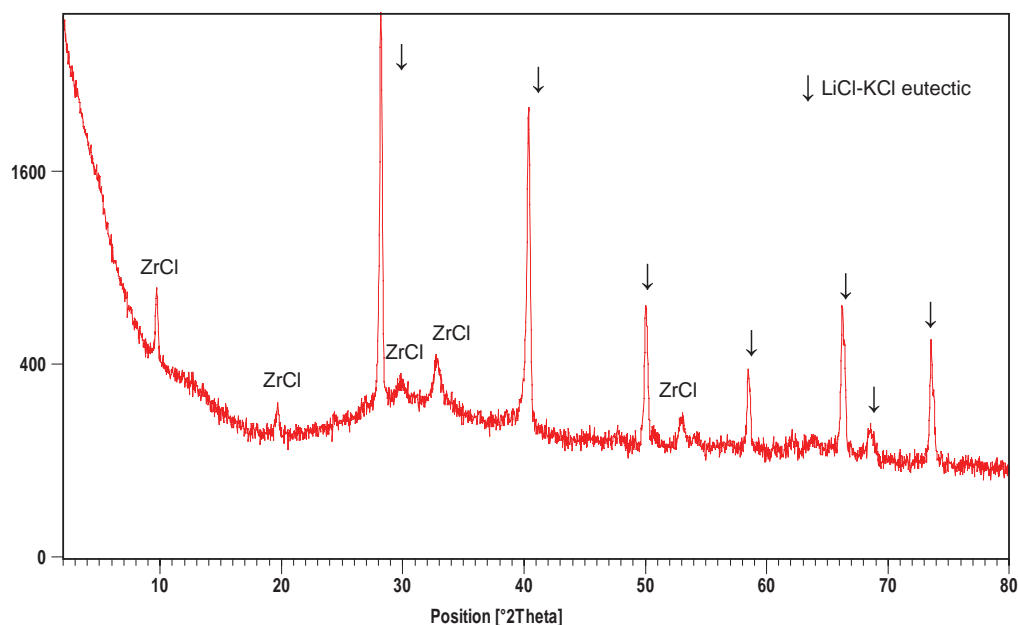

Figure 8. XRD pattern derived from the cathodic deposit obtained at 500°C with a potential of -1.2 V (vs. Ag/AgCl).

Table I. Summary of Reactions and Parameters Used to Simulate the Cyclic Voltammograms.[a]

Step	Reaction	E° / V (vs. Ag/AgCl)			k_s	K_{eq}	k_f / s^{-1}
		425°C	475°C	525°C			
1.	$Zr^{4+} = Zr^{4+*}$					1×10^3	1×10^2
2.	$Zr^{4+*} + 2e^- => Zr^{2+*}$	−1.169	−1.077	−1.079	15 s^{-1} [a]		
3.	$Zr^{2+*} + 2e^- => Zr^*$	−1.240	−1.176	−1.049	20 s^{-1} [a]		
4.	$Zr^{4+} + 3e^- = Zr^+$	−1.515	−1.470	−1.430	5 cm s^{-1} [a]		
5.	$Zr^+ = Zr^{+*}$					1×10^{10}	1×10^9
6.	$Zr^{4+} + 4e^- = Zr$	−1.55	−1.50	−1.460	10 cm s^{-1}		
7.	$Zr = Zr^*$					1×10^{15}	1×10^{10}
8.	$Zr^{+*} => Zr^{4+*} + 3e^-$	−0.864	−0.823	−0.806	500 s^{-1}		
9.	$Zr^* => Zr^{4+*} + 4e^-$	−0.852	−0.815	−0.782	500 s^{-1}		

[a]A superscripted asterisk (*) denotes an adsorbed species. Other species are assumed to be soluble. For example, in step 3, Zr^o* indicates that zirconium metal is adsorbed (present as a thin film while Zr^o in step 6 represents a very small concentration of dissolved zirconium metal at the electrode-solution interface. In step 7 virtually *all* Zr^o metal is present as a film, $K_{eq} = 10^{15}$. The maximum surface coverage used was ~10^{-8} moles.cm^{-2}. In some cases, simulations are relatively insensitive to a particular parameter, in the sense that they may be varied with the outcome resulting in little difference in agreement between simulated and experimental data, e.g., k_s value of 10 cm.s^{-1} in step 6. In the simulations, linear diffusion, Butler-Volmer electorde kinetiscs and Frumkin isotherms were assumed with no interaction between the surface confined species (a* = 0).
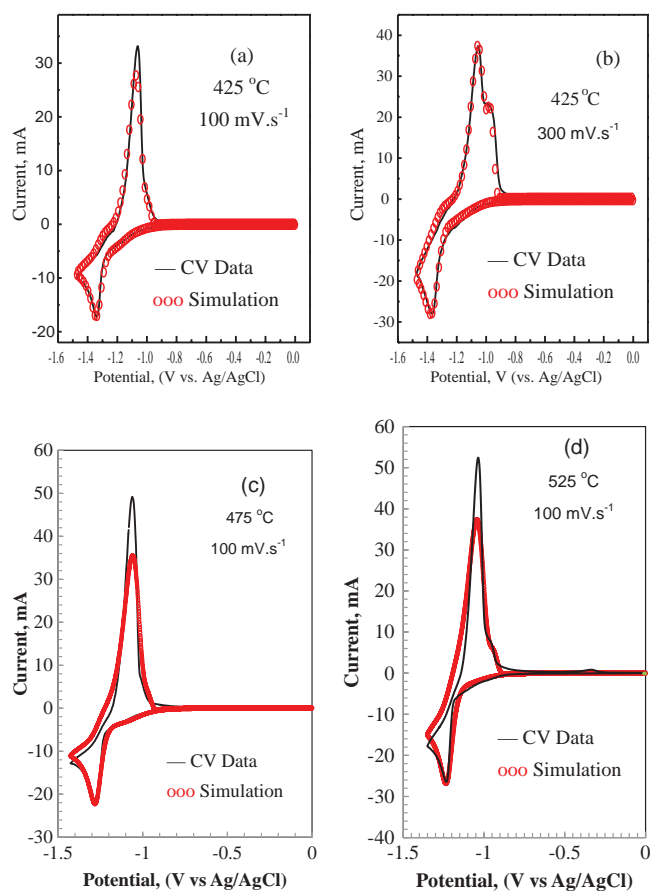

Figure 9. Comparison of simulated and experimental cyclic voltammograms obtained at designated scan rates for the reduction of Zr^{4+} in LiCl - KCl eutectic molten salt at 425°C for (a) and (b) with $[Zr^{4+}]$ = 0.027 molkg^{-1}; (c) 475°C with $[Zr^{4+}]$ = 0.0428 molkg^{-1} and (d) 525°C with $[Zr^{4+}]$ = 0.0428 molkg^{-1}. WE: W 1 mm dia. wire (electrode area: S$_{425}$ = 0.404; S$_{475}$ = 0.306 and S$_{525}$ = 0.338 cm^2); CE: - GC rod; REF, Ag/AgCl; [AgCl] = 0.75 molkg^{-1}. Diffusion coefficients (x 10^5 cm^{2}s^{-1} for all species) at 425°C = 1.25; 475°C = 1.40 and 525°C = 1.65; α = 0.5; uncompensated resistance, R_u = 0; C_{dl} = 1 × 10^{-3} F; self-interaction parameter a* = 0. See Table I for further details.

eutectic salt. The dominance of ZrCl over zirconium metal, when electrolysis is undertaken at −1.2 V (vs Ag/AgCl) agrees with the findings reported by Sakamura.[4]

Simulations of the Cyclic Voltammetry.— Simulations using a wide range of mechanisms were undertaken in an attempt to mimic the first two processes derived from reduction of Zr^{4+}. Simulations using the parameters shown in Table I provide the results shown in Figure 9. It can be seen that for both concentrations of Zr^{4+} over the temperature range from 425 to 550°C that simulations with the finally chosen mechanism successfully mimic the experimental scan rate and other characteristics. That is, excellent agreement is obtained between the simulated and experimental data under all conditions examined. In a complex mechanism such as the one proposed, the excellent accord of simulated and experimental data does not guarantee that a unique set of simulated parameters has been obtained in order to match the experimental data. Nevertheless, the excellent agreement does present some confidence that the basic features are now identified. Accordingly, the CV experimental data is now interpreted as follows: (a) the $Zr^{4+} \rightarrow Zr^{*4+}$ step is formed by a large and favorable equilibrium constant (b) the first process consists predominantly of the reduction process $Zr^{*4+} + 2e^- \leftrightarrow Zr^{*2+}$ and the simulation closely mimics the drawn out nature of this essentially surface confined process. (c) the peak shaped second reduction process represents a complex reaction with a significant diffusion component. (d) the overall reaction is irreversible.

Table I summarizes the parameters used to simulate cyclic voltammograms for the first two steps in the reduction of Zr^{4+} in LiCl - KCl eutectic molten salt at 425, 475 and 525°C and 2 Zr^{4+} concentration levels.

Table II provides peak potentials for process I$_p$C$_2$ derived experimentally. Baboian et al.[7] reported a value of −1.120 V (vs. Ag/AgCl) at 550°C which is in reasonable agreement with that −1.058 V (vs. Ag/AgCl) obtained in this work also at 550°C. Table II summarizes

Table II. Peak Potentials for E$_p$ (Process I$_p$C$_2$) and Diffusion Coefficient values (D) for Zr^{4+} determined from simulation as a function of temperature in LiCl-KCl eutectic molten salt.

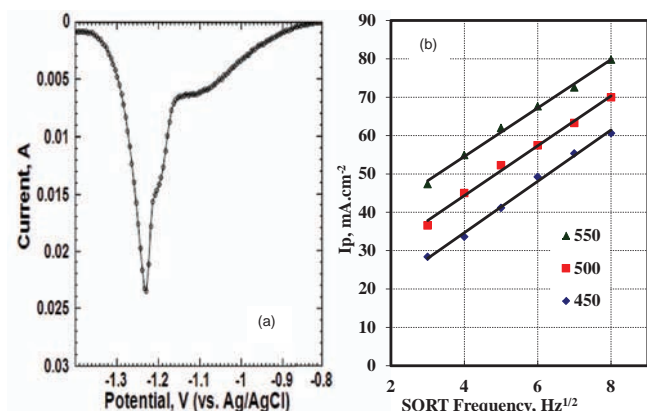| Temperature, °C	425	450	475	500	525	550
E$_p$ (I$_p$C$_2$), V (vs. Ag/AgCl)	−1.18	−1.16	−1.12	−1.09	−1.06	−1.05
D, cm^2.s^{-1}, x 10^5	1.25	1.30	1.40	1.50	1.65	1.75

Figure 10. (a) SWV at $550°C$ for Zr^{4+} (0.046 $molkg^{-1}$) in LiCl - KCl eutectic molten salt at 25 Hz with $E_{sw} = 20$ mV and $\Delta E_s = 5$ mV. WE: W 1 mm dia. wire (electrode area: $S = 0.291$ cm^2); CE: - GC rod; REF, Ag/AgCl; [AgCl] $= 0.75$ $molkg^{-1}$. (b) Dependence of the major peak current on the square root of frequency for a Zr^{4+} concentration of 0.04 $molkg^{-1}$ in LiCl - KCl eutectic molten salt at 450, 500 and $550°C$ with $E_{sw} = 20$ mV and $\Delta E_s = 5$ mV WE: W 1 mm dia. wire (area: $S = 0.272$ cm^2); CE: - GC rod; REF, Ag/AgCl; [AgCl] $= 0.75$ $molkg^{-1}$.

the diffusion coefficient values determined from simulation, which were assumed to be equal for all dissolved species. Caravaca et al.,[15] Cordova et al.[16] and Fabian et al.[11] have also reported the diffusion coefficient values in the low 10^{-5} $cm^2.s^{-1}$ range for gadolinium, neptunium and lanthanum, respectively in the LiCl-KCl electrolyte system.

Square-Wave Voltammetry of Zirconium.— Cyclic voltammetry with simulation of the theory has been the electrochemical technique of choice employed to probe the mechanism of reduction of Zr^{4+}. Square-wave voltammetry provides improved resolution and discriminates against the capacitive current and at least qualitatively can be advantageously used to probe the reaction mechanism more effectively than cyclic voltammetry.[17] SWV data were obtained with a 20 mV pulse height or amplitude (E_{sw}) and 5 mV step potential (ΔE_s) at frequencies of 9, 16, 25, 36, 49 and 64 Hz (scan rate, mVs^{-1}: 45, 80, 125, 180, 245 and 320).

Figure 10a shows a SWV for the reduction of Zr^{4+} at $550°C$. The initial adsorption dominated first reduction process $Zr^{*4+} + 2e^- \leftrightarrow Zr^{*2+}$ is again seen at about -1.1 V (vs. Ag/AgCl). However, the second predominant diffusion based process described in the cyclic voltammetry is now split into two steps with peak potentials at about -1.18 V and -1.225 V, illustrating that there is a multi-electron reduction closely spaced charge-transfer processes. Furthermore, as shown in Figure 10b the dependence of the major peak current on the square root of the frequency is linear as expected for mass transport by diffusion.[18]

Conclusions

Since zirconium is a fission product in nuclear fuels and is also used in the preparation of metallic fuels, it is important to understand its electrochemistry in pyroelectrochemical reprocessing of spent nuclear fuel. Simulation of the pyroelectrochemical complex cyclic voltammetric data was conducted and excellent agreement was obtained with a designated mechanism and experimental data at two concentrations of Zr^{4+} (0.027 and 0.043 $molkg^{-1}$) over the temperature range of 425 to $550°C$ and scan rates from 50 to 500 mVs^{-1}. Simulations indicate that the $Zr^{4+} \rightarrow Zr^{4+*}$ process has a large equilibrium constant so that the initial reduction step is predominantly a surface confined of $Zr^{*4+} + 2e^- \leftrightarrow Zr^{*2+}$ process. Simulations closely mimic the drawn out sigmoidal shaped nature of the initial reduction step. The second peak shaped reaction step is complex, but consists of combination of unresolved $Zr^{2+} + 2e^- \leftrightarrow Zr^*$, $Zr^{4+} + 4e^- \rightarrow Zr^o$, $Zr^{4+} + 3e^- \rightarrow Zr^{+*}$ reactions with a significant diffusion component. Zr^{+*} is probably ZrCl and can be reduced to Zr^o at more negative potentials. Their symmetrical shape implies that the oxidation components in cyclic voltammograms are a result of surface confined processes. SWV data provide evidence of closely spaced steps in the second reduction process.

References

1. C. Hamel, P. Chamelot, A. Laplace, E. Walle, O. Dugne, and P. Taxil, *Electrochim. Acta*, **52**, 3995 (2007).
2. M. Gibilaro, L. Massot, P. Chamelot, L. Cassayre, and P. Taxil, *Electrochim. Acta*, **55**, 281 (2009).
3. R. K. Ahluwalia, T. A. Hua, and H. K. Geyer, *Nuclear Technology*, **133**, 103 (2001).
4. Y. Sakamura, *J Electrochem Soc.*, **151**, C187 (2004).
5. T. Murakami, T. Kato, M. Kurata, and H. Yamana, *Journal of Nuclear Materials*, **394**, 131 (2009).
6. S. Ghosh, S. Vandarkuzhali, N. Gogoi, P. Venkatesh, G. Seenivasan, and B. Prabhakara Reddy, et al., *Electrochimica Acta*, **56**, 8204 (2011).
7. R. Baboian, D. L. Hill, and R. A. Bailey, *J Electrochem Soc.*, **112**, 1221 (1965).
8. G. J. Kipouros and S. N. Flengas, *J Electrochem Soc.*, **132**, 1087 (1985).
9. F. Basile, E. Chassaing, and G. Lorthioir, *J Appl Electrochem.*, **11**, 645 (1981).
10. S. Ghosh, S. Vandarkuzhali, P. Venkatesh, G. Seenivasan, T. Subramanian, and B. Prabhakara Reddy, et al., *J Electroanal Chem.*, **627**, 15 (2009).
11. C. Fabian, V. Luca, P. Chamelot, L. Massot, C. Caravaca, and G. R. Lumpkin, *J Electrochem Soc.*, **159**, F63 (2012).
12. V. Smolenski, A. Laplace, and J. Lacquement, *J Electrochem Soc.*, **151**, E302 (2004).
13. D. S. Polcyn and I. Shain, *Anal Chem.*, **38**, 370 (1966).
14. A. J. Bard and L. R. Faulkner, Electrochemical Methods, Fundamentals and Applications 2001.
15. C. Caravaca, G. De Cordoba, M. J. Tomas, and M. Rosado, *Journal of Nuclear Materials.*, **360**, 25 (2007).
16. G. Córdoba, A. Laplace, J. Lacquement, and C. Caravaca, *J. Electrochem Soc.*, **154**, F16 (2007).
17. J. C. Helfrick and L. A. Bottomley, *Anal Chem.*, **81**, 9041 (2009).
18. S. Komorsky-Lovric, M. Lovric, and A. M. Bond, *Electroanalysis*, **5**, 29 (1993).